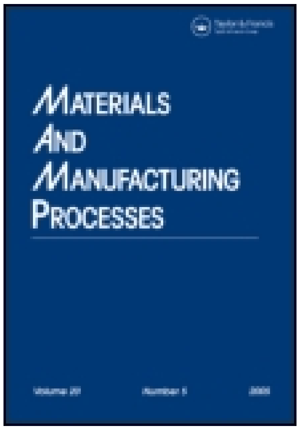

Materials and Manufacturing Processes
Publication details, including instructions for authors and subscription information:
http://www.tandfonline.com/loi/lmmp20

Characterization of Steel Welded Joints with Hybrid Projection and Capacitor Discharge Welding (CDW) Processes

F. Palano [a], S. Chiozzi [a], F. W. Panella [a] & V. Dattoma [a]
[a] Department of Engineering for Innovation, University of Salento, Lecce, Italy
Accepted author version posted online: 16 Jul 2012.Version of record first published: 26 Nov 2012.

Materials and Manufacturing Processes, 27: 1387–1391, 2012

ISSN: 1042-6914 print/1532-2475 online
DOI: 10.1080/10426914.2012.663140

Characterization of Steel Welded Joints with Hybrid Projection and Capacitor Discharge Welding (CDW) Processes

F. Palano, S. Chiozzi, F. W. Panella, and V. Dattoma

Department of Engineering for Innovation, University of Salento, Lecce, Italy

This work studies the improved hybrid Capacitor Discharge Welding process (CDW), based on projection welding principles applied to stainless steel AISI 304.

The innovative idea is to modify the igniting points geometry on the section to be welded and optimize the weld characteristics in order to guide the local fusion processes more uniformly on the whole area and enhance the weld properties. Eight different profile geometries for the contact surfaces have been realized in order to evaluate the geometry influence on joints quality and according to process parameters influence. The mechanical behavior of the welds has been verified with static characterization at room temperature and fatigue tests for welded samples with the better observed microstructure.

Keywords AISI 304; CDW; Fatigue behavior; Technology; Tensile test.

Introduction

The capacitor discharge welding (CDW) process with multipoint welding profile awakened the interest of mechanical industries; it represents an effective tool for components repair, such as engine parts and aeronautical turbine blades [1, 2].

The present article deals with new developments of the CDW process, referred particularly to AISI 304 butt joints, on the bases of previous works [3, 4].

The CDW process is a welding technique which requires the simultaneous application of elevate pressure and temperatures; it is based on resistance welding method and technologically realized through intense current pulses as for projection welding [5].

The current values are particularly elevated and the application times much smaller than those employed in common resistance welding, as well as the final junction is not achieved through consecutive welded spots, but the whole section is jointed in a single weld. The energy required for the intense CDW discharge is furnished by large capacitors battery [3–5]; moreover, the weld shape is defined by the geometry of the parts and not affected by material singularities or surface discontinuities, typical of spot welds.

This research focuses the attention on the multipoint CDW technique (MCDW) conceived by the authors [2], which represents an hybrid version of simple capacitor discharge welding and classic projection welding [5]. It is proposed with the aim to joint larger surfaces and free from defects typical of CDW, such as porosity and lack of fusion.

Received September 20, 2011; Accepted January 16, 2012

Address correspondence to F. Palano, Department of Engineering for Innovation, University of Salento, Lecce, Italy; E-mail: fania.palano@unisalento.it

In this work, the butt-weld cylindrical specimens are machined to adopt a trapezoidal contact profile on one of the parts to be welded [1, 3]. Welding tests have been realized investigating eight different contact geometries and examining also the technological parameters (energy and applied force) and the output measures (peak current and joint mutual penetration). The geometrical and technological factors are combined to improve the welding efficiency, mainly in terms of mechanical strength.

In order to assess the new joint geometries, inspection of all the welded joints for external defects, optical observation of the welded section, and room temperature tests for mechanical characterization were done.

CDW process advances and welding tests

According to authors' works [2, 3] and in relation to scientific literature data [6, 7], small diameter welded bars can be achieved up to 6 mm with cylindrical single igniter geometry. For wider surfaces, distributed igniting points have to be used, to produce a round weld and a more uniform process on the whole section, experimenting the multipoint version of the CDW process [1, 3].

Alternatively to contact geometries considered in previous experiences [1–4], a new multipoint type solution is proposed; an innovative trapezoidal contact geometry (Fig. 1) with suited welding parameters have been studied since they are suggested by previous works [8, 9] in which CDW simulations are performed.

The trapezoidal profile [10] are shaped only on one of the two welding edges and the characteristic dimensions are showed in Fig. 1: the tooth width l and depth h; the pitch p between consecutive teeth; tooth sides inclination α. This new contact profile is proposed with the following purposes: reducing manufacturing costs, increasing

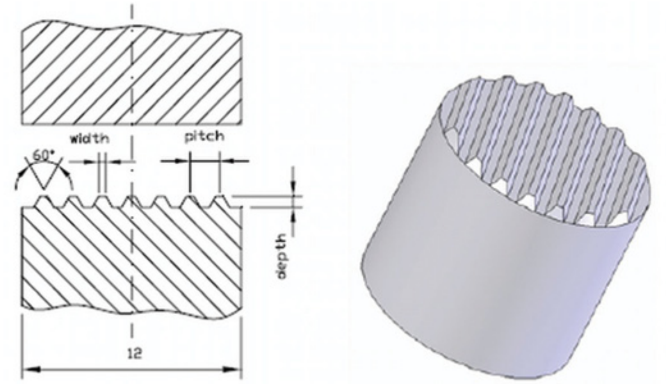

FIGURE 1.—2D and 3D views of the new adopted contact profile, based on simple trapezoidal shape (color figure available online).

melted material, raising the weld bead thickness, and improving the joint ductility to avoid defect presence.

It is possible to define the igniters total volume *V* to be melted in the weld line and the first contact surface ratio *C* between the two parts during the discharge.

To evaluate the influence of these two factors on CDW outcome, eight different contours, characterized by a combination of the parameters *l, h*, and *p*, but all with the same α (60°) value, have been realized (Table 1).

The limit values of these parameters have been selected on the base of finite element method (FEM) simulations [8, 9] and previous experiments [4] to ensure the correct heat input in the material to be welded. A total number of 64 specimens were welded.

A first welding session, which had the intent to verify the initial FEM input welding values, was performed and the visual inspection of the obtained joints is immediately done.

A second welding session had the aim to optimize the process factors, by performing tensile tests on all joints with different applied energy so that to identify the optimal process configuration. The experimental procedure for the joints achievement was similar to the previously implemented one [10], and special equipment was employed for the parts assembly and electrical conductivity.

The process parameters have been modified from time to time for each geometry between the limits of 15 KJ (lower values are ineffective) and 45 KJ (maximum machine power) in several discharges, generally in the number of 5.

TABLE 1.—Geometric data of the different contact profiles.

Profile	*l* (mm)	*h* (mm)	*p* (mm)	*V* (mm^3)	*C* (%)
1	0.4	0.6	1.6	30.03	22.48
2	0.4	0.6	1.72	23.31	15.17
3	0.2	0.6	2	18.16	9.19
4	0.4	0.2	1.54	7.1	23.96
5	0.2	0.2	2	3.59	9.88
6	0.4	0.4	1.6	17.14	23.23
7	0.2	0.4	2	9.67	9.54
8	0.2	0.4	1.33	13.72	13.61

TABLE 2.—Input parameters and welding outcome for the best specimens for each profile.

Profile	F (kN)	E_1 (kJ)	E_2 (kJ)	E_3 (kJ)	E_4 (kJ)	E_5 (kJ)	t (ms)	I (kA)	I_i (kA · s)
1	30	3	45	25	2	2	8	215.1	1,350
2	30	3	45	5	2	2	10	189.9	1,281
3	30	3	40	5	2	2	9	191.2	1,172
4	25	3	45	5	2	2	10	206.3	1,304
5	25	3	45	15	2	2	8	195.6	1,208
6	30	3	45	5	2	2	8	217.8	1,361
7	30	3	40	30	2	2	9	193.4	1,123
8	30	3	40	20	2	2	8	218.3	1,431

The symbols are: F is the compressive force applied; E_i is the electrical energy of the ith discharge; M_d is the parts mutual distance; t is the welding time; I_p is the maximum current peak; and I_i is the integrated current over time.

The fundamental discharges are only the second and the third one from 15 to 40 kJ, since a single discharge of maximum power is insufficient for the whole section to be welded; other discharges (from 2 to 5 kJ) are of lower intensity for post-heating purposes and were previously studied to reduce the cooling rate and redistribute precipitates [2–4]. All specimens have been welded by applying a force in the range 25–40 kN.

In Table 2, the input parameters employed in each discharge and the output welding outcome furnished by the machine are summarised for the best specimens related to each profile.

Adopting a single discharge and limited force values to reduce misalignment, the specimen seemed to be partially welded; so it was decided to apply a minimum of two main discharges on other specimens. The joints resulted in better welds and showed a slight bulge, probably due to the employment of excess energy.

All the welding sessions data were satisfactory, since they allowed to identify the input parameters and weld outcome which guarantee the best performance for every profile. An important factor which characterizes the weld quality is the radial swelling on the joints and the related weld depth *Md*, which is a direct index of enough melted metal in the weld layer, leading to better ductility behavior. It has been demonstrated that a consistent raise of *Md* due to higher force and discharged energies is observed. It is to be established if a greater *Md* factor has a positive effect on joint strength, considering also that the CDW process requires to limit the induced deformations as more as possible.

MECHANICAL CHARACTERIZATION

Tensile and Fatigue Tests

All samples present resistant section having 8 mm diameter and gauge length 10 mm. A servo-hydraulic machine MTS 810 with a 100 kN load cell has been adopted. All the 40 tests have been executed at room temperature, with crosshead rate 0.1 mm/min. Base metal has been preventively tested, deducing the stress-strain curve ($\sigma_R = 841.2$ mpA, $\sigma_{p0.2} = 595$ MPa, E = 10,170 MPa, A = 76.34%) to establish the mechanical decay of the welded material respect to it.

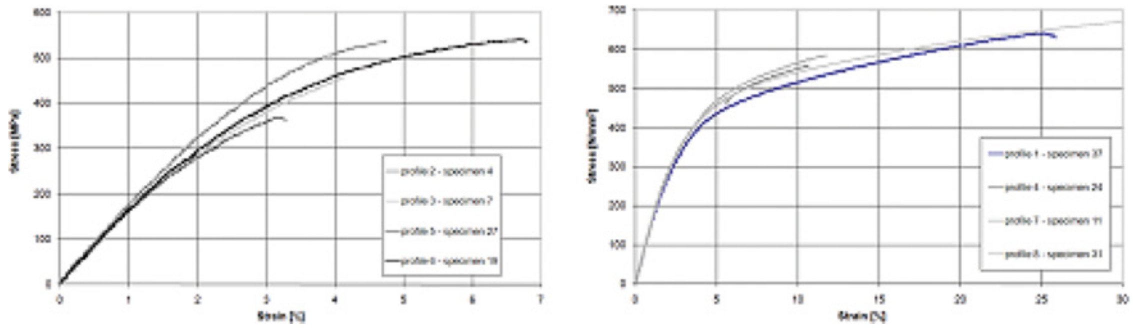

FIGURE 2.—Stress-strain curves for the best specimen of each profile (color figure available online).

The following structural data have been computed for each specimen: rupture stress σ_R; yielding stress $\sigma_{p0.2}$; Young modulus E; and rupture elongation A. In Fig. 2 the stress-strain curves related to each profile are reported for more representative tests.

The results vary in considerable manner, not only for different profiles, but also for the same one, as function of the adopted welding parameters. Particularly, a low elongation value with poor plastic behavior can be observed for most of the welded samples: it is mainly due to the considerable thinness of the weld beads in the order of 0.2–0.5 mm.

To analyze all the tensile tests results, the rupture stress values are statistically reported in Table 3 for each profile. The marked superiority of profiles 1 and 8, in terms of strength and ductility, can be immediately observed. Particularly, the welding parameters combination corresponding to profile 8 allows to achieve 80% strength and nearly 40% rupture elongation respect to base metal. This result establishes the pitch *p* of the contact profile is to be as smaller as possible (below 1.6 mm) and with enough profile height *h*, over 0.4 mm.

The result is even more remarkable if it is noticed that no specimen overcomes 15% of base material ductility, by excluding the mentioned profiles.

From a comparison between this new data and those previously published [2], similar outcomes are achieved in terms of σ_{Rmean}. A more significant goal is pursued, since the welded surface is double and the multipoint profile may arise more solidification defects. This fact suggests the better adaptability of contour 8 to CDW process. At the contrary, the inefficiency of profile 5 is emerged: evidently, it is characterized by low igniters height *h* and too high pitch *p* to guarantee sufficient weld quantity to create a consistent weld bead. In fact, no specimen gains 400 MPa ultimate stress threshold.

TABLE 3.—Best welded joints mechanical properties.

Profile	σ_{Rmax} [MPa]	σ_{Rmean} [MPa]	Standard deviation [MPa]	Number of static tested specimens
1	642.5	512.4	96.1	4
2	536.8	412.6	133,4	6
3	454.7	304.2	129,4	5
4	558.5	446.1	99,1	6
5	397.1	375.1	19,4	3
6	541.4	493.9	31,9	4
7	585.5	470.3	61,3	7
8	670.3	569.2	68,2	4

Encouraging results are observed for tests on profiles 1, 4, 6, and 7, for which the calculated mean stress are all greater than 450 MPa, confirmed by data dispersion to be sufficiently small. Contrasting conclusions seem to arise on profiles 2 and 3 results, for which mean strength values are lower than 350 MPa, with data very scattered around the mean values.

A sufficient number of specimens for fatigue tests has been welded corresponding to profile 6 (profile 8 specimens were not enough); the profile has been chosen also on the base of good depth values measured on specimens after welding. Profile 6 specimens were subjected to high cycle fatigue tests with load ratio $R = \sigma_{min}/\sigma_{max} = 0.1$, since the welds are expected to work under tensile conditions. The results are described by the Wöhler curve reported in Fig. 3.

The fatigue properties are characterized by high stress level; the Wöhler curve is settled between 10^4 and 10^6 cycles with alternate stresses σ_a positioned between 208 MPa and 123 MPa. The fatigue curve has a flat trend. The fatigue limit for 2×10^6 cycles is greater than $100\,N/mm^2$: the exact values of the fatigue limits at 10^6 cycles could not be processed, but the minimum stress value is expected to be around 114 MPa.

Data Analysis

The joints strength depending on input geometry and technological parameters can be analyzed to better identify the optimal values; the efficiency of the CDW technique in terms of repeatability and welded product quality is to be to guaranteed for future applications. The mutual distance for instance, *Md* factor, is associated with evident improvement of the joint mechanical strength, indicating the *Md* value to be a good control indicator for mass production processes.

Concerning the igniter geometry influence and adopting statistic elaboration on all welding data, useful indications can be raised: in Fig. 4a, the results are resumed, showing the process efficiency for each profile as percentage of relative welds resistance with respect to two reference thresholds (430 and 500 MPa). Contact profile

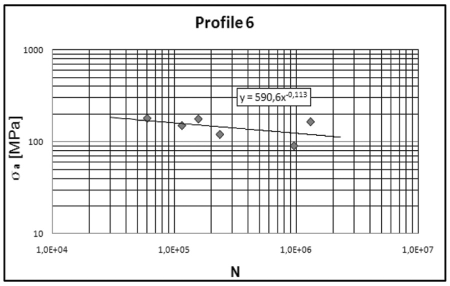

Specimen	σ_a [MPa]	N
1	150.818	114969
2	120.654	235634
3	90.491	956712
4	165.899	13100288
5	180.981	59660
6	177.934	157075
Base metal [11]	217	2000000

FIGURE 3.—Wöhler curve for profile 6 and fatigue data for each specimen.

8 is proved to be a good selection, together with profiles no. 1 and 6 with lower efficiency values. Other significant relations between the joints strength and the contact profiles geometry are displayed with diagrams in Fig. 4b, where rupture stresses versus the important profile factors V and C is illustrated.

From Fig. 4b, it is clear the total igniter volume V is to be larger than 10 mm^3, to assure sufficient melted metal quantity for the achievement of high joint strength. At the same time, the contact area percentage C holds a more relevant role. In fact, for higher igniters heights h, a mechanical collapse occurs before or during the first discharge to take place. Consequently, a great igniter volume is not always associated to good welding quality, while the contact surface is more useful. The best performance is gained with contours having C values higher than 13%; this signifies that the igniters height h must be greater than 0.4 mm. The pitch p on the other way is preferred up top 1.6 mm, given that a tendency to cold welding defects and loss of ductility is likely to be observed in the region between two consecutive igniters. Regarding the technological parameters influence, for the total input energy E_{tot} an optimal range emerged between 60 and 70 kJ, to be shared in the two main discharges. This tendency is particularly visible for profiles having heights h equal to 0.6 mm: greater igniters depth requires more energy to reach complete fusion of the parts. In any case, the optimal force values to be applied are found to be over 30 kN, as confirmed in other works [9]. Generally, F value must be as higher as possible, respecting the igniters compression strength limits; values greater than 35 kN are unadvisable, since the risk to provoke the igniters collapse before the discharge occurs.

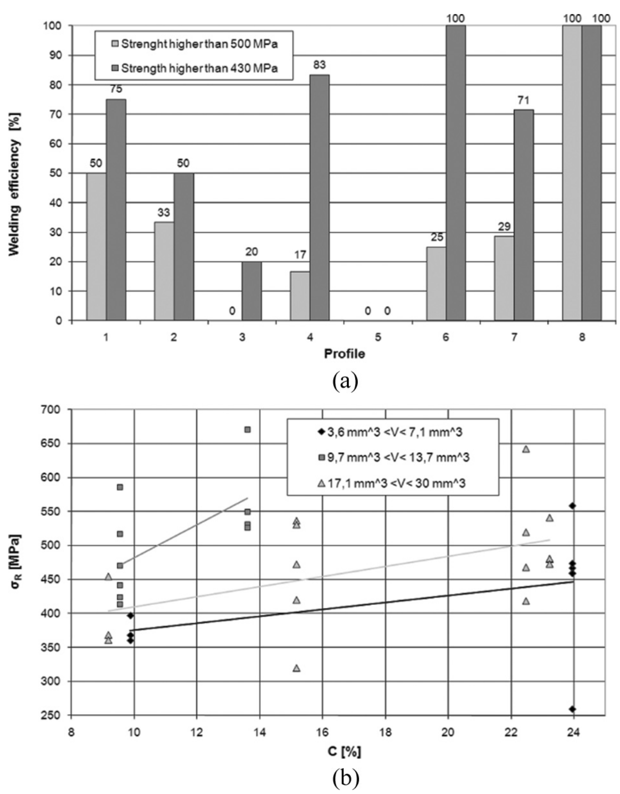

FIGURE 4.—a) Welding efficiency of joints statically resistant respect to reference values, for each profile. b) σ_R trend as function of C for different ranges of V values.

Micrographic Analysis

The microstructure has been studied through optical microscope observation. Interesting results are reported that describe metallurgical effects on few selected welds in the longitudinal section, along the contact profile.

Figure 5a shows contact profile example of poor profile 5 weld: lack of adhesion has been noticed in the internal zone beside the base material on both the two parts of the joint, each of 1.5 mm of length, in the zone between two consecutive igniters. This is the typical CDW effect and gives an evident indication of profile 5 inefficiency, due to excessive gap between the igniters. The micrographic inspection allows distinguishing the welded joint, characterized by total lack of precipitates, whose streaks are well visible on the base material.

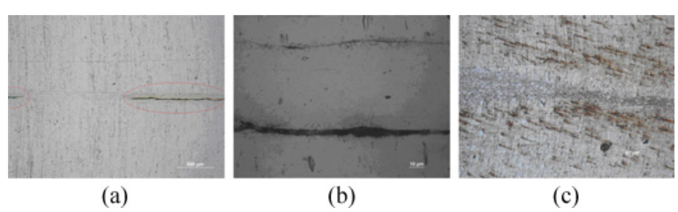

FIGURE 5.—a) Micrograph specimen 26 (50x). b) Micrograph specimen 26 (1000x). c) Micrograph specimen 17 (200x) (color figure available online).

Moreover, in correspondence of the joint edge it is possible to notice dendritic ramification in the thermal flux direction (Fig. 5b).

Finally, an example of profile 6 is reported in Fig. 5c: it is possible to notice good grains elongation that follows the thermal rate. Even though the melted metal distribution is not entirely uniform, welded layer appears sufficiently coherent with the base material also at joint extremities, with sufficient thickness exempt from macrodefects.

Conclusions

In this work, CDW process in multipoint configuration and applied to axial-symmetrical geometries has been completely characterized and improved with optimization of the contact profile. Mechanical tests correlated with micrographic inspections have shown contact profiles which guarantee the best mechanical performances and technological parameters that give an optimal efficiency of the process have been selected. Mechanical strength and ductility resulted satisfactory.

Special attention has been spent to monitoring the control parameter *Md* because it has been found to correlate well the joints mechanical strength for high *Md* values.

The process dependence, in terms of efficiency, on two basic geometrical parameters has been verified: total igniter volume V and first contact percentage area C have been analyzed. The contact surface holds a relevant role for the achievement of high joint strength.

Finally, it was possible to improve the input parameters, by applying two main discharges and total energy E_{tot} between 60 and 70 kJ; the optimum force F can be placed around 30 kN. Results are encouraging, because the CDW process's potentialities are significant and can ensure the technique efficiency in terms of repeatability and quality of the weld product. Achieved conclusions can be used as bases for extending with success CDW technology on mechanical components of the same material, but more complex than the axial-symmetric discussed in this work.

References

1. Chiozzi, S.; Dattoma, V.; Panella, F.W. Capacitor discharge welded bars of Inconel 718 and TiAl6V4 superalloys under fatigue. *Materials and Design* **2008**, *29*, 839–851.
2. Palano, F.; Panella, F.W.; Dattoma, V. Characterization of aeronautical engine parts joined by CDW welding process. *Proc. IMechE Part G J. Aerosp. Eng.* **2010**, *223*, 11–22.
3. Dattoma, V.; Palano, F.; Panella, F.W. Mechanical and technological analysis of AISI 304 butt joints welded with capacitor discharge process. *Materials and Design* **2010**, *31*, 176–184.
4. Casalino, G.; Panella, F.W. Microstructural analysis of AISI 304 bars welded with high speed pulsed discharges. *J. Mater. Process. Technol.* **2007**, *191*, 149–152.
5. Alley, R.L. Capacitor discharge stud welding. In *ASM Handbook, Vol. 6, Welding, Brazing and Soldering*; ASM International: Materials Park, OH, 1991.
6. Wilson, R.D. Explore the potential of capacitor discharge welding. *Adv. Mater. Process.* **1994**, *145*, 93–94.
7. Devlietan, J.H.; Venkataraman, S. Rapid solidification of stainless steels by capacitor discharge welding. *Welding Journal Research Supplement* **1988**, *67*, 111–118.
8. Casalino, G.; Panella, F.W. Numerical simulation of multipoint capacitor discharge welding of AISI 304 bars. *Proc. IMechE Part B J. Eng. Man.* **2006**, *220*, 647–655.
9. Cavaliere, P.; Dattoma, V.; Panella, F.W. Numerical analysis of multipoint CDW welding process on stainless AISI304 steel bars. *Comput. Mater. Sci.* **2009**, *46*, 1109–1118.
10. Chiozzi, S.; Palano, F.; Panella, F.W. Studio di giunti in acciaio 304 saldati con tecnica ibrida CDW a proiezione. In *Proceedings of XXXVII AIAS Congress*, Rome, Italy, 2008.
11. Lampman, S. Fatigue and fracture properties of stainless steel. In *ASM Handbook, Vol. 19 Fatigue and Fracture*; ASM International: Materials Park, OH, 1996.